SCIENCE CHINA
Earth Sciences

• RESEARCH PAPER •

March 2012 Vol.55 No.3: 488–494
doi: 10.1007/s11430-011-4354-3

High-resolution anisotropy of magnetic susceptibility record in the central Chinese Loess Plateau and its paleoenvironment implications

LIU WeiMing[1,2*] & SUN JiMin[1]

[1]*Key Laboratory of Cenozoic Geology and Environment, Institute of Geology and Geophysics, Chinese Academy of Sciences, Beijing 100029, China;*
[2]*Key Laboratory of Mountain Hazards and Earth Surface Process, Institute of Mountain Hazards and Environment, Chinese Academy of Sciences, Chengdu 610041, China*

Received March 9, 2011; accepted June 29, 2011; published online January 12, 2012

We analyze high-resolution anisotropy of magnetic susceptibility (AMS) of the loess-paleosol successions at Luochuan, central Chinese Loess Plateau, in order to investigate the AMS characteristics and their climatic implications. Our results indicate a normal sedimentary magnetic fabric for almost of all samples, characterized by minimum susceptibility axes grouped in an almost vertical direction. Magnetic foliation and anisotropy degree show upwards decreasing trend due to decreasing post-depositional compaction. Magnetic lineations show no preferred directions and thus cannot indicate paleowind patterns. AMS parameters at Luochuan are controlled by particle size, pedogenesis, and sedimentary compaction. The high peaks of magnetic foliation and anisotropy degree of L2, L3, L6, L9, and L15 correspond to the coarse particle sizes of these loess beds, indicating the grain-size dependence of AMS.

Chinese loess, anisotropy of magnetic susceptibility, Quaternary, Luochuan

Citation: Liu W M, Sun J M. High-resolution anisotropy of magnetic susceptibility record in the central Chinese Loess Plateau and its paleoenvironment implications. Sci China Earth Sci, 2012, 55: 488–494, doi: 10.1007/s11430-011-4354-3

Chinese loess is one of the best terrestrial climatic records over the last 2.6 Ma [1–3], characterized by alternations of loess and palaeosol layers. The loess layers accumulated during glacial periods with enhanced cold/dry winter monsoon, whereas paleosol layers developed during interglacial periods with enhanced warm-humid summer monsoon. Therefore, the alternations of loess and paleosol layers represent alternating East Asian monsoon circulations on glacial-interglacial time scales [4, 5]. Numerous studies of Chinese loess have used various climatic parameters including particle size, magnetic parameters, geochemistry, and mineralogy to infer past climatic variability [6–9]. For example, the anisotropy of magnetic susceptibility (AMS) has been used to infer paleowind patterns on the Chinese Loess Plateau.

The pioneering AMS work on the Chinese Loess was done by Heller et al. [10]. Subsequent work of Liu et al. [11] found that re-deposited loess has a higher degree of anisotropy ($1.032 \leqslant P \leqslant 1.064$) than wind blown deposits ($1.002 \leqslant P \leqslant 1.032$). Afterwards more AMS studies have been performed to solve a series of problems of loess, such as prevailing wind patterns [12–14], possible deformation or disturbance [15] and identification re-deposited or primary loess [16]. Among these studies, some researchers suggested that the maximum principal axis (K_1) of loess AMS indicated dust transport directions [12, 14, 17, 18]. However, some studies indicated that the AMS of loess may be more

*Corresponding author (email: liuwm@imde.ac.cn)

complex than previously thought. For example, the loess profile of Lingtai, K_1 of AMS record indicates NE-SW and NW-SE orientations since last interglacial, which probably corresponded to paleowind directions [19]. For the youngest loess in Poland and western Ukraine, however, mean minimum axes of AMS but not K_1 were considered reflecting the prevailing palaeowind directions [13]. In addition, recent work of Zhu et al. [20] indicates that K_1 is chaotically distributed and cannot be used to determine paleowind directions at three loess profiles on Chinese Loess Plateau. Therefore it is still necessary to study the relationship between the loess AMS and paleowind direction, in despite of these previous attempts. In this study, we systematically investigate the AMS parameters of the classical Quaternary loess-soil successions at Luochuan, in order to test if the AMS at this section indicates paleowind directions.

1 Sampling and measurements

The Luochuan loess section (35.7°N, 109.4°E) is located in the central Chinese Loess Plateau (Figure 1), it was previously divided into four parts—the Wucheng (oldest), the Lower Lishi, the Upper Lishi, and the Malan [1]. More detailed field observations subdivided it into thirty three couplets of loess (L) and soil (S) [23]. This section was first reported by Liu [24] and further studied by many researchers [23, 25–27]. In the field, 1284 oriented hand samples were collected with a sampling interval of 10 cm, of which six samples were from the upper part of the Tertiary Red Clay. In the laboratory, oriented samples were cut into cubic specimens (2 cm×2 cm×2 cm) for AMS measurements.

To determine the magnetic mineralogy and grain-size distribution, rock magnetic measurements were made for four typical loess and paleosol samples. Temperature-dependent susceptibility (χ-T) curves were measured using a MFK1-FA Kappabridge equipped with a CS4 high- temperature furnace (Agico Ltd., Brno) between room temperature and 700°C in an argon atmosphere. Hysteresis loops, isothermal remanent magnetization (IRM) acquisition curves and back field demagnetization curves were measured with a Princeton Measurements Corp. Model 3900 Vibrating Sample Magnetometer (VSM). The AMS of all samples was measured by using a KLY-4s Kappabridge (Agico Ltd., Brno) with an automated sample handling system. Each sample was rotated through three orthogonal planes. The AMS of a sample can be illustrated in terms of an ellipsoid with three orthogonal principal axes corresponding to the maximum, intermediate, and minimum principal (K_1, K_2 and K_3) axes, respectively. The susceptibility ellipsoid was calculated by the 15-position orientation scheme suggested by Jelínek & Kropáček [28]. The orientations of the mean magnetic susceptibility ellipsoid with the associated uncertainties were determined by the tensor variability [29]. All these magnetic measurements were performed at the Paleomagnetism and Geochronology Laboratory of the Institute of Geology and Geophysics, Chinese Academy of Sciences.

Various parameters have been defined to describe the shape and anisotropy of the magnetic susceptibility ellipsoid. The major AMS parameters examined in this study are: magnetic susceptibility (K) = (K_1+K_2+K_3)/3, and mass normalized as χ; lineation (L) = K_1/K_2; foliation (F) = K_2/K_3; degree of AMS (P) = K_3/K_1; and shape parameter of AMS (T) = $(2n_2-n_1-n_3)/(n_1-n_3)$; where n_1, n_2 and n_3 are lnK_1, lnK_2 and lnK_3, respectively. The declination and inclination of K_1 (K_2 and K_3) is denoted by Dec-K_1 (K_2 and K_3) and Inc-K_1 (K_2 and K_3). Parameters F_{12} and F_{23} are used to evaluate the statistical significance of the lineation and the foliation, while the parameter of E_{12} represents the half-angular uncertainty in the direction of K_1 within the magnetic foliation plane.

2 Results

2.1 Rock magnetic results

The χ-T curves for all samples exhibit a major decrease at

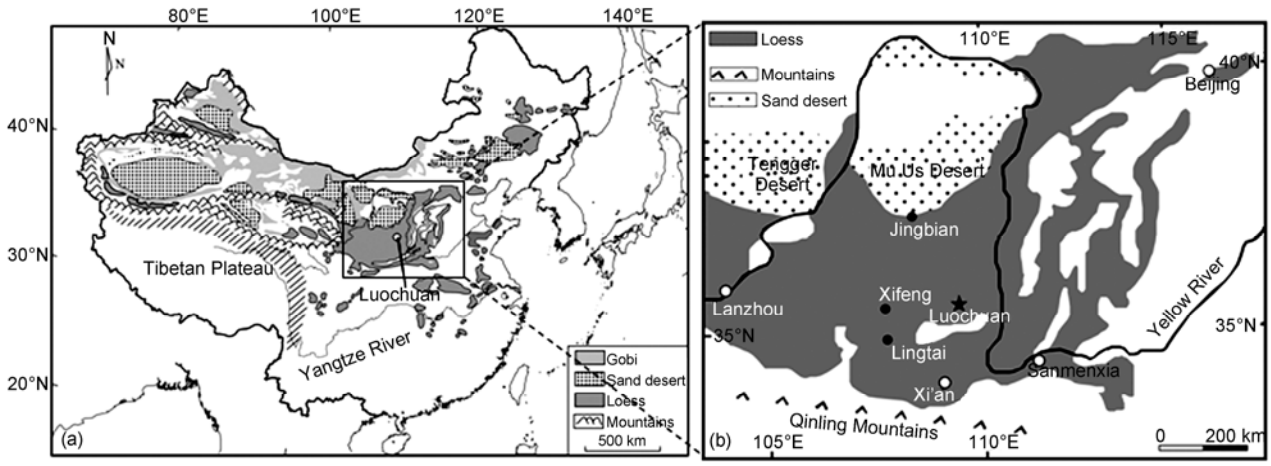

Figure 1 Sketch map showing loess distributions in China as well as the location of the Luochuan section (modified from Sun & Zhu [21] and Guo et al. [22]).

about 585°C, which indicates the presence of magnetite (Figure 2(a)–(d)). The heating curves also show a χ hump near 300°C. The slight increase of χ below 300°C was generally attributed to the gradual unblocking of fine ferromagnetic particles (near the superparamagnetic/single domain boundary) [32] or the release of stress upon heating [33]. The steady decreases after 300°C is generally interpreted as the conversion of metastable maghemite to weakly magnetic hematite [32]. The heating curve for the L6 sample is almost flat up to 400°C. This temperature independence is indicative of the coarse-grained nature of the detrital magnetite particles [34]. Another notable characteristic is the χ after cooling is always several times higher than the initial values before heating, which is generally attributed to the neoformation of magnetite grains from iron-containing silicates/clays [35] such as chlorite [36], or due to the formation of magnetite by reduction as a result of the burning of organic matter [36].

After the removal of a paramagnetic contribution, hysteresis loops for all the samples show similar characteristics. They are almost closed before 300 mT (Figure 2(e)–(h)), consistent with dominant soft magnetic minerals (e.g., magnetite, maghemite) [37, 38]. Each IRM acquisition curve reaches approximate saturation at about 300 mT (Figure 2(i)), which indicates that the major proportion is consistently carried by low coercivity magnetic carriers (e.g., magnetite, maghemite). The stepwise demagnetization of SIRM using a DC back field also shows a lower coercivity of remanence (H_{cr}) for all samples (Figure 2(j)). In the Day plot, all samples are almost indistinguishable in pseudo-single-domain (PSD) range (Figure 2(k)).

2.2 AMS results

The majority of samples have statistically significant L and F, with F_{12}>4, E_{12}<20° (Figure 3(a)) and F_{23}>10 (Figure 2(c)). Figure 2(b) shows the F_{12} has a weak positive correlation with χ, probably due to the increasing measurement

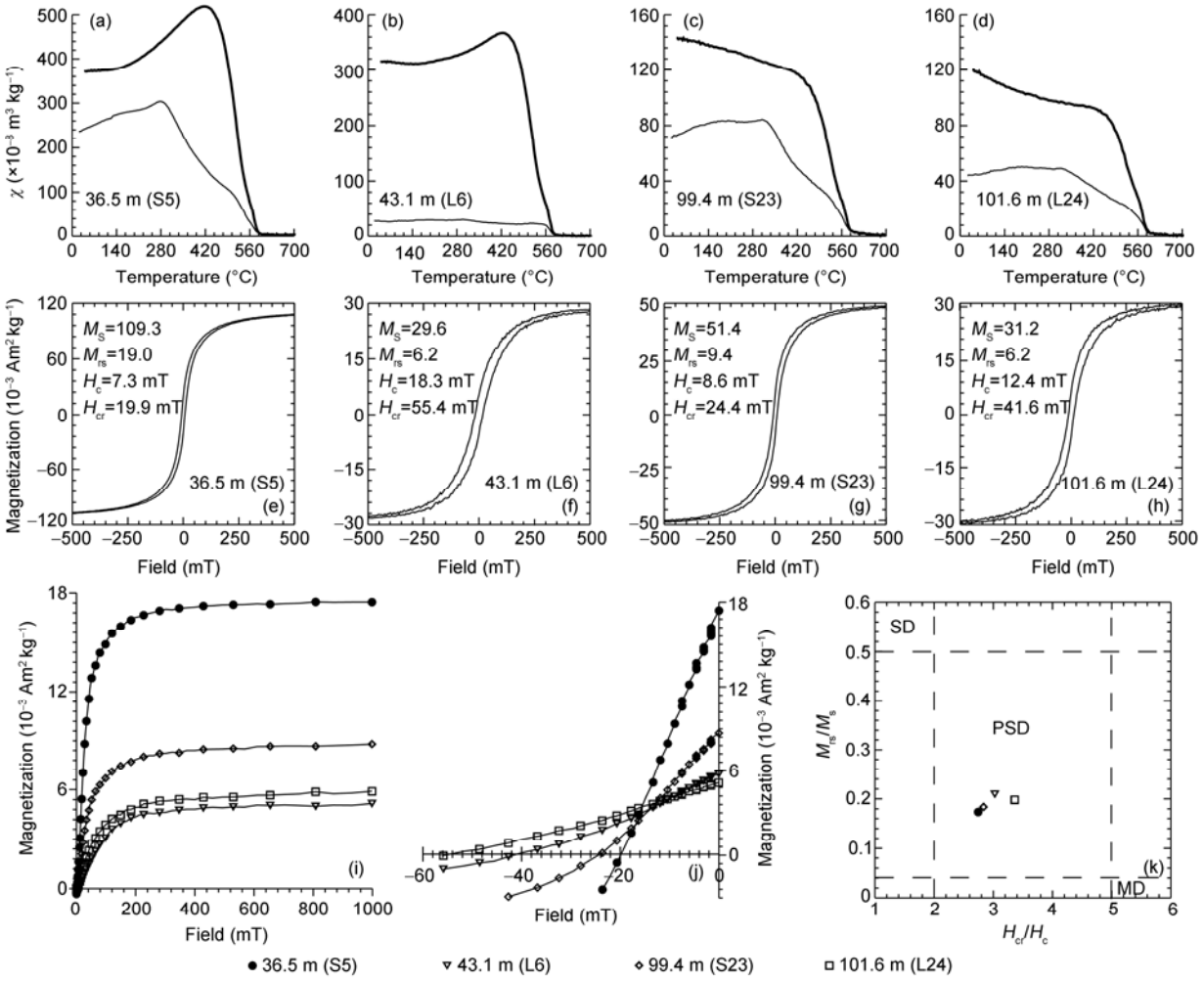

Figure 2 Rock magnetism results for the Luochuan section. (a)–(d) Temperature-dependent susceptibility curves. Thick (thin) lines indicate heating (cooling) runs. (e)–(h) Hysteresis loops, after subtraction of the paramagnetic contribution. (i) Isothermal remanent magnetization acquisition curves. (j) Back-field demagnetization of IRM. (k) Hysteresis ratios plotted on a Day plot [30, 31].

errors with lower magnetic susceptibility. 124 samples of $F_{12} < 4$ or $E_{12} > 20°$ were rejected (as indicated by the shadow in Figure 3(a)) to reduce noisy directions.

The values of F are between 1 and 1.025 (Figure 3(d)), whereas values of P were between 1.001 and 1.027 (Figure 3(e)). The shape parameter (T) of the AMS ellipsoids was generally located in the oblate region, except several samples that fall into the prolate area (Figure 3(f)).

3 Discussions

3.1 AMS affected by post-depositional sedimentary compaction

There are apparent long-term increasing trends in P and F from the top to the bottom of the section, which parallel the variable trend of the dry bulk density (Figure 4). Bulk density is defined as the ratio of mass and volume of sample and depends greatly on the degree of the post-depositional compaction. P and F are about 1.015 at the bottom, and gradually decrease to 1.002 at the top, meanwhile the dry bulk density decreases from 1.65 to 1.2 g cm^{-3}. Therefore, the increase trend of F and P towards the bottom of the section is mainly caused by compaction. The earlier accumulated loess was overlain by the subsequently deposited younger loess leading to increased interlocking of the grains and a decrease in the void ratio. The sedimentary compaction leads to a preferred orientation of particles, due to passive rotation in a matrix that can be easily deformed [39]. In this context, the compaction leads to the increased F and P as the accumulation thickness increase.

There are no remarkable AMS differences between loess and paleosol layers at this section except the remarkable peaks of F and P at L2, L3, L6, L9 and L15 (Figure 4(b)–(d)). The averaged L, F and P of all loess layers are 1.0010, 1.008 and 1.009, respectively, being similar to that of the all paleosol layers. This is different from the other paleoclimatic proxies (e.g. magnetic susceptibility and grain size). Therefore, the L, F and P cannot reflect the glacial-interglacial climatic changes at Luochuan.

3.2 Are paleowind directions can be inferred by AMS at Luochuan?

The paleowind direction and strength can be inferred from alignments of K_1 and K_3 of AMS for aeolian deposition [40, 41]. Weak wind would produce the K_1 parallel to the direction of wind, whereas strong wind would align the K_1 perpendicular to the wind direction [41].

In this study, we find that Dec-K_1 is not only randomly distributed for all samples (Figures 4(g) and 5), but also for L1 (Figure 5(d)), the Upper Lishi (Figure 5(e) and (f)), and other coarse-grained loess units (L9, L15 and L24) (Figure 5(g), (h) and (i)). The direction of K_3 is also randomly distributed (Figures 4(h) and 5). Therefore, AMS cannot be used to determine paleowind directions at Luochuan, being similar to other loess sites [20, 42, 43].

The random distributions of main principal axes of AMS

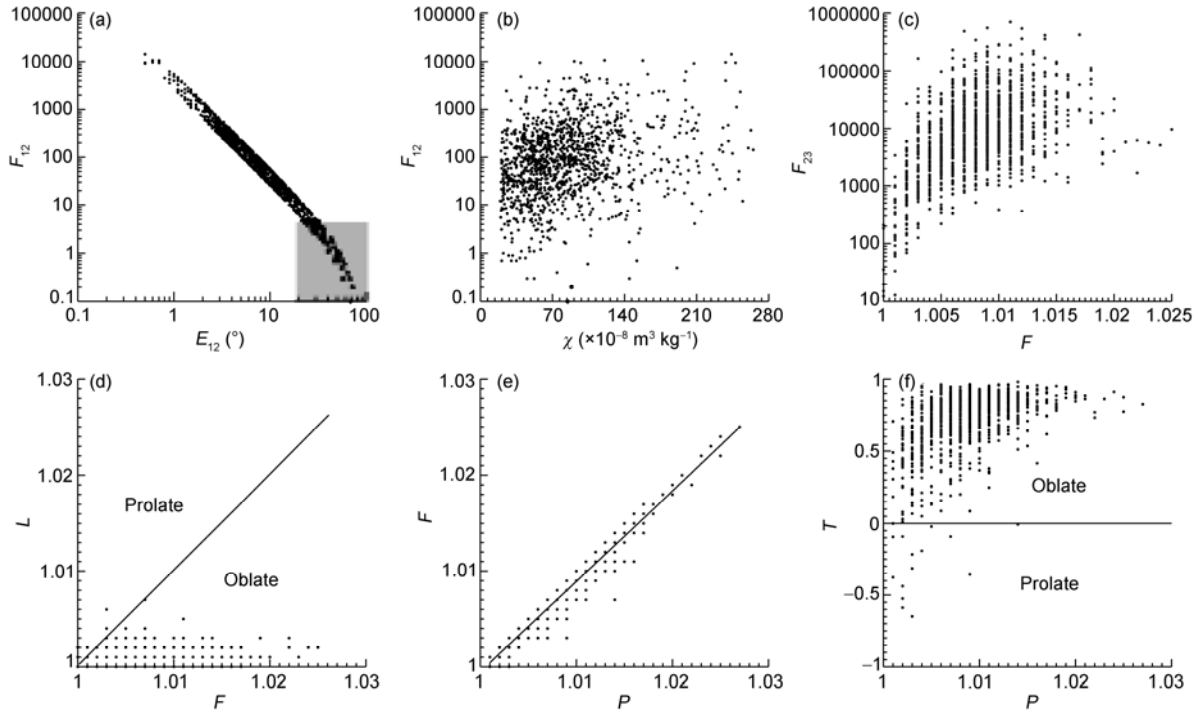

Figure 3 Statistical significance, angular uncertainties and relationships of the AMS parameters. The shadow indicates the samples with $F_{12} < 4$ and $E_{12} > 20°$.

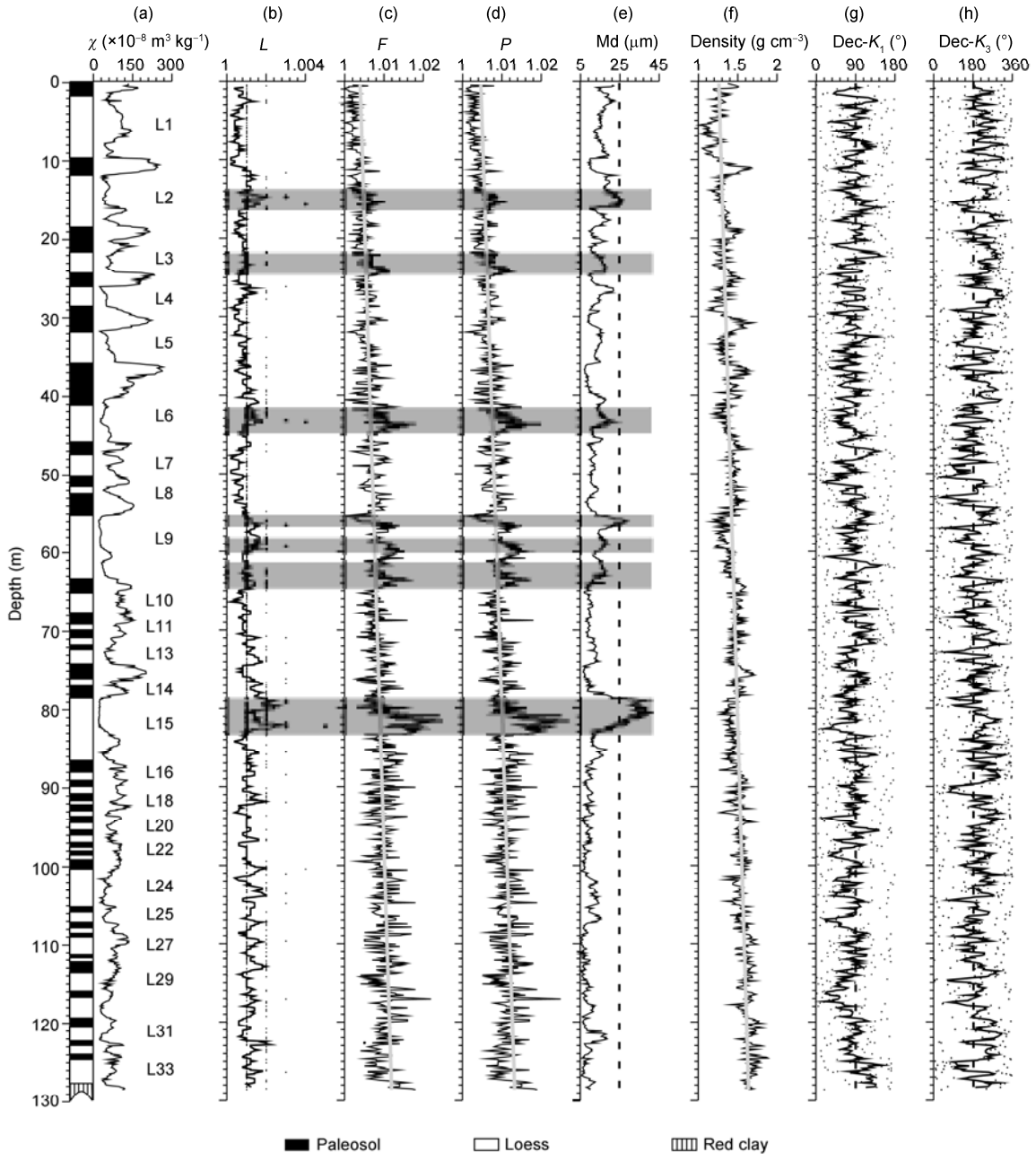

Figure 4 Magnetic susceptibility, *L*, *F*, *P*, Md, dry bulk density, Dec-K_1, and Dec-K_3 versus depth at Luochuan. Data of *L*, Dec-K_1, and Dec-K_3 are smoothed by using a five-point running mean. The bold red lines in *F*, *P* and dry bulk density show the increasing trends towards bottom. The gray shadows mark the remarkable peaks of *F*, *P* and particle size.

(Figures 4 and 5) can be affected by fine particle size, post-depositional alternations, sedimentary compaction, and local topography. Firstly, the particle size of Chinese loess is at least partially related to the wind strength [1, 42]. The studied Luochuan section is located in the central Loess Plateau. The distance to the dust provenance is relatively long. As a matter of fact, wind strength that transporting eolian dust decreases with the increasing distance, leading to the dominant fine silt particles (median size generally less than 25 μm, Figure 4(e)) at Luochuan. The dominant fine particle size reflects weak winds resulting in the poor magnetic lineation. The relationship between particle size and AMS can be further supported by the fact that the coarse loess beds of L2, L3, L6, L9, L15 correspond to the remarkable peaks of *L*, *F*, and *P* (Figure 4). Secondly, dust whenever accumulates undergoing subsequent post-depositional alterations. The climate pattern of the Loess Plateau is controlled by the East Asian monsoon. The warm and humid summer monsoon weakens northwestly leading to the declined post-depositional alterations from southeast to northwest. In this sense, the central Loess Plateau (where Luochuan section is located) underwent stronger pedogene-

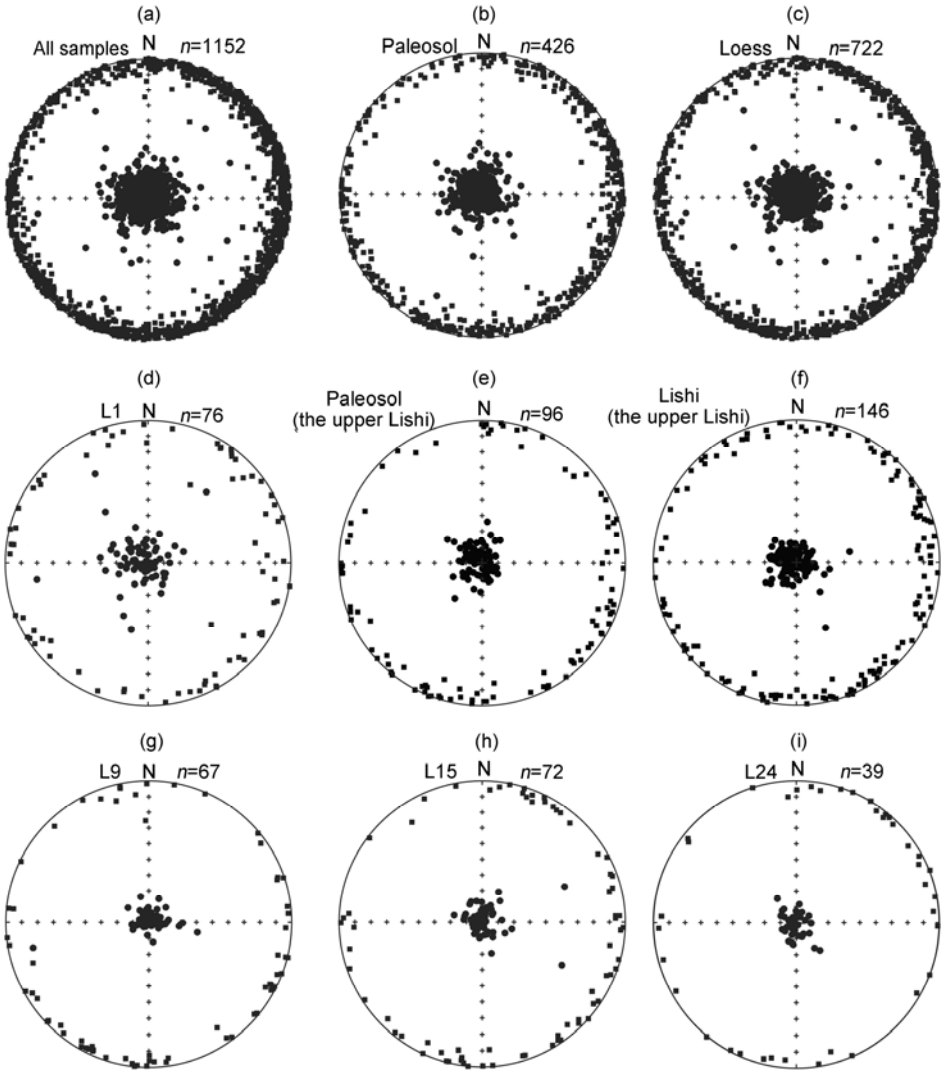

Figure 5 Equal-area projections of AMS principal axes for all samples, soils, and loess beds, respectively. Squares and circles represent K_1 and K_3 axes.

sis compared with that in the northern Loess Plateau. The pedogenesis can disturb the alignments of particles. Thirdly, the sedimentary compaction as demonstrated by the temporal variations of AMS can also affect the alignments of the particles.

Actually, the roles of the above those factors act together at a given loess site, for instance, the loess deposits in the southern Loess Plateau not only have relatively finer particle size but also undergo stronger pedogenesis and have less porosity. In this context, the ideal sites for reconstructing paleowind directions are located in the northwestern Loess Plateau where the coarse sandy loess undergoes weak pedogenesis. This can explain why AMS of the sandy loess in the northern Loess Plateau can reflect paleowind directions [44].

4 Conclusions

Based on high-resolution AMS measurements of the Quaternary loess-soil successions at Luochuan, we have the following conclusions:

(1) The parameters of AMS indicate oblate shapes of AMS ellipsoid. The temporal variation trends of F and P are quite similar. Both parameters show long-term upwards decreasing trend that are mostly related to sedimentary compaction.

(2) Dec-K_1 is randomly distributed for all samples at Luochuan implying that the AMS of loess deposits in the central Loess Plateau cannot be used to reconstruct paleowind directions.

(3) The AMS of loess deposits are controlled by multiple factors including particle size, pedogenesis, and sedimentary compaction. Considering the spatial gradients of particle size and climate within the Loess Plateau, future AMS studies for wind pattern reconstructions should focus on the northern and northwestern Loess Plateau.

This work was supported by the National Basic Research Program of Chi-

na (Grant No. 2010CB833400), Chinese Academy of Sciences (Grant Nos. KZCX2-YW-Q09-06-04, KZCX2-YW-130), and National Natural Science Foundation of China (Grant No. 40830104). We thank Qingsong Liu and Shiling Yang for useful discussions. We also thank the two anonymous reviewers for their helpful comments.

1 Liu T S. Loess and Environment. Beijing: China Ocean Press, 1985
2 An Z S. The history and variability of the East Asian paleomonsoon climate. Quat Sci Rev, 2000, 19: 171–187
3 Ding Z L, Derbyshire E, Yang S L, et al. Stacked 2.6-Ma grain size record from the Chinese loess based on five sections and correlation with the deep-sea δ^{18}O record. Paleoceanography, 2002, 17, 3: 1003, doi: 10.1029/2001PA000725
4 An Z S, Liu T, Lu Y, et al. The long-term paleomonsoon variation recorded by the loess-paleosol sequence in Central China. Quat Int, 1990, 7-8: 91–95
5 Liu T S, Ding Z L. Chinese loess and the paleomonsoon. Annu Rev Earth Planet Sci, 1998, 26: 111–145
6 An Z S, Kukla G J, Porter S C, et al. Magnetic susceptibility evidence of monsoon variation on the Loess Plateau of central China during the last 130000 years. Quat Res, 1991, 36: 29–36
7 Xiao J, Porter S C, An Z, et al. Grain size of quartz as an indicator of winter monsoon strength on the Loess Plateau of Central China during the last 130000 yr. Quat Res, 1995, 43: 22–29
8 Chen J, An Z, Head J. Variation of Rb/Sr ratios in the loess-paleosol sequences of Central China during the last 130000 years and their implications for monsoon paleoclimatology. Quat Res, 1999, 51: 215–219
9 Ji J, Balsam W, Chen J. Mineralogic and climatic interpretations of the Luochuan loess section (China) based on diffuse reflectance spectrophotometry. Quat Res, 2001, 56: 23–30
10 Heller F, Beat M, Wang J, et al. Magnetization and sedimentary history of loess in the central Loess Plateau of China. In: Liu T S, ed. Aspects of Loess Research. Beijing: China Ocean Press, 1987. 147–163
11 Liu X M, Xu T C, Liu T S. The Chinese loess in Xifeng, II. A study of anisotropy of magnetic susceptibility of loess from Xifeng. Geophys J Int, 1988, 92: 349–353
12 Lagroix F, Banerjee S K. Paleowind directions from the magnetic fabric of loess profiles in central Alaska. Earth Planet Sci Lett, 2002, 195: 99–112
13 Nawrocki J, Polecho O, Boguckij A, et al. Palaeowind directions recorded in the youngest loess in Poland and western Ukraine as derived from anisotropy of magnetic susceptibility measurements. Boreas, 2006, 35: 266–271
14 Bradak B. Application of anisotropy of magnetic susceptibility (AMS) for the determination of paleo-wind directions and paleo-environment during the accumulation period of Bag Tephra, Hungary. Quat Int, 2009, 198: 77–84
15 Zhu R, Liu Q, Pan Y, et al. Identifying the origin of the magnetic directional anomalies recorded in the Datong loess profile, northeastern Chinese Loess Plateau. Geophys J Int, 2006, 164: 312–318
16 Clarke M L. A comparison of magnetic fabrics from loess silts across the Tibetan front, Western China. Quat Proc, 1995, 4: 9–26
17 Lagroix F, Banerjee S K. The regional and temporal significance of primary aeolian magnetic fabrics preserved in Alaskan loess. Earth Planet Sci Lett, 2004, 225: 379–395
18 Liu Q, Yu Y, Deng C, et al. Enhancing weak magnetic fabrics using field-impressed anisotropy: Application to the Chinese loess. Geophys J Int, 2005, 162: 381–389
19 Zhu R, Liu Q, Jackson M. Paleoenvironmental significance of the magnetic fabrics in Chinese loess-paleosols since the last interglacial (< 130 ka). Earth Planet Sci Lett, 2004, 221: 55–69
20 Zhu Y, Zhou L, Zhang S. A preliminary study on anisotropy of magnetic susceptibility of the late Pliocene-early Pleistocene aeolian eposits in northern China (in Chinese with English abstract). Quat Sci, 2007, 27: 1009–1014
21 Sun J M, Zhu X K. Temporal variations in Pb isotopes and trace element concentrations within Chinese eolian deposits during the past 8 Ma: Implications for provenance change. Earth Planet Sci Lett, 2010, 290: 438–447
22 Guo Z, Berger A, Yin Q, et al. Strong asymmetry of hemispheric climates during MIS-13 inferred from correlating China loess and Antarctica ice records. Clim Past, 2009, 5: 21–31
23 Sun J M, Liu T S. Stratigraphic evidence for the uplift of the Tibetan Plateau between similar to 1.1 and similar to 0.9 Myr ago. Quat Res, 2000, 54: 309–320
24 Liu T S. Composition and Texture of Loess. Beijing: Science Press, 1966
25 Heller F, Liu T S. Magnetostratigraphical dating of loess deposits in China. Nature, 1982, 300: 431–433
26 Kukla G, An Z S. Loess stratigraphy in Central China. Palaeogeogr Palaeoclimatol Palaeoecol, 1989, 72: 203–225
27 Bloemendal J, Liu X. Rock magnetism and geochemistry of two Plio-Pleistocene Chinese loess-palaeosol sequences—Implications for quantitative palaeoprecipitation reconstruction. Palaeogeogr Palaeoc- limatol Palaeoecol, 2005, 226: 149–166
28 Jelínek V, Kropáček V. Statistical processing of anisotropy of magnetic susceptibility measured on groups of specimens. Stud Geophys Geod, 1978, 22: 50–62
29 Hext G R. Estimation of second-order tensors, with related tests and designs. Biometrika, 1963, 50: 353–373
30 Day R, Fuller M, Schmidt V. Hysteresis properties of titanomagnetites: Grain-size and compositional dependence. Phys Earth Planet Inter, 1977, 13: 260–267
31 Dunlop D J. Theory and application of the Day plot (M_{rs}/M_s versus H_{cr}/H_c) 1. Theoretical curves and tests using titanomagnetite data. J Geophys Res, 2002, 107, B3, doi: 10.1029/2001jb000486
32 Liu Q, Deng C, Yu Y, et al. Temperature dependence of magnetic susceptibility in an argon environment: Implications for pedogenesis of Chinese loess/palaeosols. Geophys J Int, 2005, 161: 102–112
33 Liu Q, Torrent J, Morras H, et al. Superparamagnetism of two modern soils from the northeastern Pampean region, Argentina and its paleoclimatic indications. Geophys J Int, 2010, 183: 695–705
34 Deng C, Shaw J, Liu Q, et al. Mineral magnetic variation of the Jingbian loess/paleosol sequence in the northern Loess Plateau of China: Implications for Quaternary development of Asian aridification and cooling. Earth Planet Sci Lett, 2006, 241: 248–259
35 Hunt C P, Banerjee S K, Han J, et al. Rock-magnetic proxies of climate change in the loess-palaeosol sequences of the western Loess Plateau of China. Geophys J Int, 1995, 123: 232–244
36 Ao H, Dekkers M J, Deng C, et al. Palaeclimatic significance of the Xiantai fluvio-lacustrine sequence in the Nihewan Basin (North China), based on rock magnetic properties and clay mineralogy. Geophys J Int, 2009, 177: 913–924
37 Deng C, Zhu R, Verosub K L, et al. Mineral magnetic properties of loess/paleosol couplets of the central Loess Plateau of China over the last 1.2 Myr. J Geophys Res, 2004, 109, B1, doi: 10.1029/2003jb002532
38 Roberts A P, Cui Y, Verosub K L. Wasp-waisted hysteresis loops: Mineral magnetic characteristics and discrimination of components in mixed magnetic systems. J Geophys Res, 1995, 100: 17909–17924
39 Hus J. The magnetic fabric of some loess/palaeosol deposits. Phys Chem Earth, 2003, 28: 689–699
40 Hrouda F. Magnetic anisotropy of rocks and its application in geology and geophysics. Surv Geophys, 1982, 5: 37–82
41 Tarling D, Hrouda F. The Magnetic Anisotropy of Rocks. London: Chapman & Hall, 1993
42 Matasova G, Petrovsky E, Jordanova N, et al. Magnetic study of Late Pleistocene loess/palaeosol sections from Siberia: Palaeoenviro- nmental implications. Geophys J Int, 2001, 147: 367–380
43 Zhu R, Shi C, Suchy V, et al. Magnetic properties and paleoclimatic implications of loess-paleosol sequences of Czech Republic. Sci China Ser D-Earth Sci, 2001, 44: 385–394
44 Sun J M, Ding Z L, Liu T S, et al. Primary application of magnetic susceptibility measurement of loess and paleosols for reconstruction of winter monsoon direction (in Chinese). Chin Sci Bull, 1995, 40: 1976–1978